Vol. 13, pp. 1–11 (2016)
doi: 10.2142/biophysico.13.0_1

Biophysics and Physicobiology
https://www.jstage.jst.go.jp/browse/biophysico/

Regular Article

Switching of the positive feedback for RAS activation by a concerted function of SOS membrane association domains

Yuki Nakamura[1,2], Kayo Hibino[3], Toshio Yanagida[2] and Yasushi Sako[1,2]

[1]*Cellular Informatics Laboratory, RIKEN, Wako, Saitama 351-0198, Japan*
[2]*Nanobiology Laboratories, Graduate School of Frontier Biosciences, Osaka University, Suita, Osaka 565-0871, Japan*
[3]*Laboratory for Cell Signaling Dynamics, RIKEN QBiC, Suita, Osaka 565-0874, Japan*

Received November 10, 2015; accepted December 11, 2015

Son of sevenless (SOS) is a guanine nucleotide exchange factor that regulates cell behavior by activating the small GTPase RAS. Recent *in vitro* studies have suggested that an interaction between SOS and the GTP-bound active form of RAS generates a positive feedback loop that propagates RAS activation. However, it remains unclear how the multiple domains of SOS contribute to the regulation of the feedback loop in living cells. Here, we observed single molecules of SOS in living cells to analyze the kinetics and dynamics of SOS behavior. The results indicate that the histone fold and Grb2-binding domains of SOS concertedly produce an intermediate state of SOS on the cell surface. The fraction of the intermediated state was reduced in positive feedback mutants, suggesting that the feedback loop functions during the intermediate state. Translocation of RAF, recognizing the active form of RAS, to the cell surface was almost abolished in the positive feedback mutants. Thus, the concerted functions of multiple membrane-associating domains of SOS governed the positive feedback loop, which is crucial for cell fate decision regulated by RAS.

Key words: EGF-RAS-MAPK system, fluorescence microscopy, cell signaling, single-molecule imaging

The SOS-RAS interaction regulates the transduction of growth factor signals, governing many cellular processes, including proliferation, differentiation, metabolic control, and morphological changes [1]. The association of growth factors with their receptors induces tyrosine phosphorylations in the cytoplasmic domain of the receptors, which are then recognized by cytoplasmic phosphotyrosine-binding proteins [2]. In the cytoplasm, SOS forms a complex with one of these phosphotyrosine-binding proteins, GRB2 [3]. Therefore, upon the activation of growth factor receptors, SOS is recruited from the cytoplasm to the plasma membrane through the association between the activated receptors and GRB2. On the plasma membrane, SOS stimulates the exchange of a guanine nucleotide molecule that is bound to RAS [4]. The GDP-bound form of RAS (RAS-GDP) is inactive, and the exchange of the GDP molecule to GTP converts RAS into its active form (RAS-GTP) [5]. The spontaneous release of guanine nucleotide from RAS occurs too slowly to have any physiologically effects, and RAS activation is facilitated by guanine nucleotide exchange factors (GEFs), such as SOS [6]. Because the concentration of GTP in the cytoplasm is much higher than that of GDP, the release of GDP essentially results in the association of GTP with RAS molecules. The GTP on the RAS molecule is then hydrolyzed to GDP, inactivating RAS.

SOS is a protein comprising six domains, each of which has a specific function (Fig. 1A). From the N-terminus, SOS contains a histone fold (H) domain, a Dbl-homology (DH) domain, a pleckstrin homology (PH) domain, a RAS-exchange motif (REM) domain, a Cdc25 domain, and a GRB2-binding (G) domain. The H domain has a conserved, positively charged patch, and interacts electrostatically with the plasma membrane [7–9]. The DH domain interacts with the REM domain to regulate the association between SOS and RAS-GTP on the REM domain. The Cdc25 domain is the catalytic site that interacts with RAS-GDP. The PH domain associates with phosphatidylinositol 4,5-bisphosphate and phosphatidic acid

Corresponding author: Yasushi Sako, Cellular Informatics Laboratory, RIKEN, 2 -1 Hirosawa, Wako, Saitama 351-0198, Japan.
e-mail: sako@riken.jp

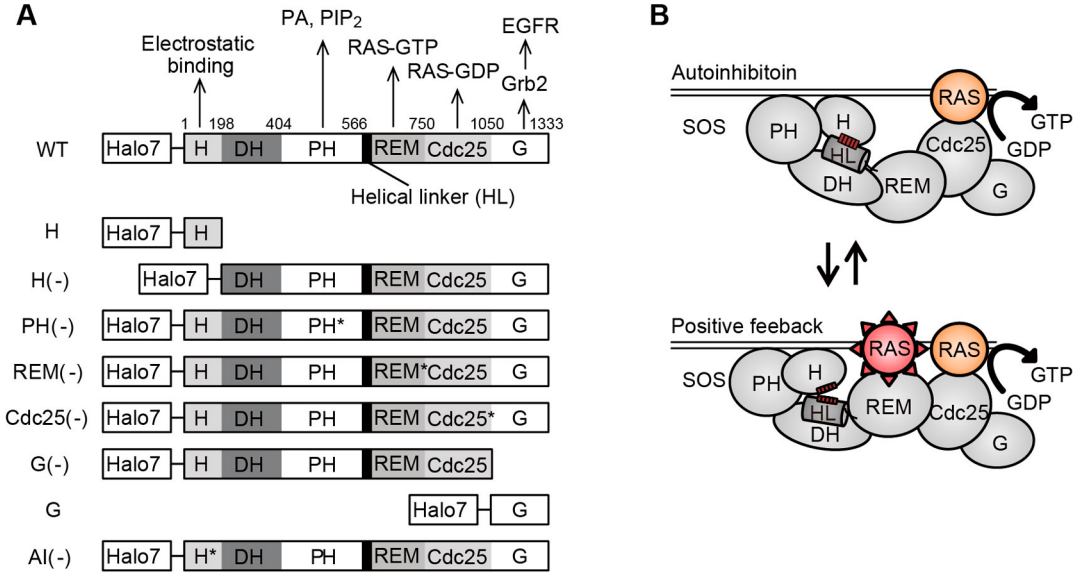

Figure 1 SOS structure and positive feedback of RAS activation

(A) The domain structures of Halo7-tagged SOS and its mutants. WT is wild-type human SOS1 tagged with Halo7 at the N-terminus. Membrane components that interact with each domain are indicated in the WT structure. H, H(–), G(–), and G are deletion mutants, Δ198–1333, Δ1–191, Δ1066–1333, and Δ1–1049, respectively. Others are point mutants lacking the membrane-associating function of the domain indicated by the asterisk: PH(–) is a quadruple mutant, K456E/R459E/H475E/R479E; REM(–) is a triple mutant, L687E/R688A/W729E; Cdc25(–) and AI(–) are single mutants, F929A and D140A, respectively. (B) SOS/RAS positive feedback. In the autoinhibited state, the DH domain disturbs the interaction between the REM domain and RAS-GTP due to the association between the H domain and helical linker (HL) between the DH and REM domains When the H domain is released from HL, RAS-GTP can interact with the REM domain to stimulate GDP/GTP exchange on RAS associating with the Cdc25 domain. Thus, it is believed that high densities of RAS-GTP on the plasma membrane result in the amplification of RAS-GTP formation (a positive feedback loop).

in the plasma membrane [10,11]. The C-terminal G domain is the GRB2-binding site [12]. Thus, SOS contains five possible membrane-interacting domains: H, PH, REM, Cdc25, and G. The H and PH domains directly associate with membrane lipids. The REM and Cdc25 domains associate with RAS on the membrane. The G domain associates with phosphorylated forms of membrane receptors via Grb2.

Recent *in vitro* studies have suggested that the SOS-mediated activation of RAS is regulated by positive feedback [13], i.e., the association of RAS-GTP with the REM domain of SOS allosterically promotes the nucleotide exchange of RAS-GDP at the catalytic site in the Cdc25 domain (Fig. 1B). An *in vitro* study [14] demonstrated that in the presence of RAS^{Y64A}-GTP, mutants of SOS in the REM domain (L687E/R688A and W729E) lowered the nucleotide dissociation rate of RAS by a factor of ten relative to that of the wild-type [15]. RAS^{Y64A}-GTP binds to the allosteric (positive feedback) site in the wild-type REM domain but not to the catalytic site. A combination of *in vitro* and *in silico* study suggested that this positive feedback mechanism sustains RAS activation, eliciting memory of antigens in lymphocytes [16]. It is thought that in the inactive conformation of SOS, the association of RAS-GTP with REM is disturbed by steric hindrance attributable to the interaction between the DH and REM domains. In addition, an intramolecular interaction between the H domain and the helical linker, which presents between PH and REM domains, is thought to be important to maintain the inactive autoinhibited conformation of SOS, because a mutation in the helical linker (R552G) increases the nucleotide dissociation rate of RAS [8] and because the mutated helical linker does not interact with the H domain [17]. This gain-of-function mutant was identified in Noonan syndrome patients. A previous study has shown that RAS is excessively activated by this mutation when cells are stimulated with epidermal growth factor (EGF) [18]. It has been suggested that the membrane recruitment of the H domain is coupled to the release of SOS autoinhibition. Thus, coordination between the domains of SOS seems to be required to activate SOS molecules and regulate the positive feedback of RAS activation.

These results were mostly obtained through *in vitro* biochemical experiments and X-ray crystallographic studies of the segments of SOS and RAS. The GEF activity of SOS molecule with a truncation of the G-domain was analyzed in a reconstructed system using fluorescence microscopy [19]. However, it remains unclear how the positive feedback mechanism functions, and, especially, how the positive feedback is regulated in living cells. In this study, we observed single-molecules of SOS on the plasma membrane of living HeLa cells to determine the dynamics and kinetics of SOS behaviors in response to EGF stimulation. Single-molecule imaging is a useful technique for tracking the dynamics of a

small number of molecules [20] and analyzing the kinetics of molecular interactions [21,22] in living cells. Comparing the behaviors of wild-type and mutant SOS molecules (Fig. 1A), we found that concerted function of the SOS membrane association domains is necessary to switch on the positive feedback between SOS and RAS, which crucially regulates the activation of RAS in living cells.

Materials and Methods

Construction of Plasmids

The Halo7 plasmid vector was constructed by exchanging EGFP in pEGFP-C2 vector (#6083-1, BD Biosciences Clontech) for Halo7, derived from the FN19K HaloTag T7 SP6 Flexi Vector (Promega). Halo7-SOS cDNA was constructed by inserting the hSOS1 fragment from pCGN-HA-hSos1 [3] into the Halo7 vector with PCR. SOS point mutants were constructed by directory introducing mutations into Halo7-SOS using the QuikChange Lightning Site-Directed Mutagenesis Kit (Agilent Technologies) and PrimeSTAR® Max DNA Polymerase (Takara). The truncation mutants were cloned into Halo7-SOS with the appropriate primer sets. The domain structures of the wild-type and mutant SOS molecules used in this study are shown in Figure 1A. The construction of GFP-RAF cDNA has been described in Hibino *et al.*, 2003 [23].

Preparation of Cells

HeLa cells were maintained in Dulbecco's modified Eagle's medium, supplemented with 10% fetal bovine serum, at 37°C under 5% CO_2. The cells were sub-cultured on glass coverslips and transfected two days before the experiments with cDNA using Lipofectamine® LTX with Plus™ Regent (Invitrogen). Next, the cells were cultured for 16 h in minimal essential medium (MEM) without phenol red but supplemented with 1% BSA. Immediately before the experiments, the cells were incubated for 15 min with 100 nM HaloTag® TMR Ligand (Promega) in culture medium. Staining with the TMR ligand was saturated under this condition. The cells were washed with Hank's balanced salt solution and MEM, and observed in MEM that contained 5 mM PIPES (pH 7.4) and 1% BSA. The remaining TMR molecules that were non-specific for SOS were less than 6.5% of the specific staining (Supplementary Fig. S2A). Under the microscope, cells were stimulated with 100 ng/ml (final concentration) EGF (Preprotech) at 25°C.

Single-molecule Imaging

Single-molecules of Halo7-tagged proteins that were labeled with TMR were observed in living cells using a home-made total internal reflection fluorescence microscope (TIRFM), based on an inverted microscope (IX81, Olympus) [24]. The cells were illuminated with a 555-nm solid-state laser (GCL-075-555, CrystaLaser) through an objective (PlanApo 60× NA=1.49; Olympus). The fluorescence images of single molecules were acquired at an emission wavelength of 560–680 nm using an electron-multiplying CCD camera (ImagEM, Hamamatsu Photonics) at a frame rate of 20 s^{-1}. Single-molecule imaging of GFP-RAF was performed using the same microscope system as described in Hibino *et al*, 2011 [21]. The cytoplasmic fluorescence intensities of TMR-SOS and GFP-RAF were measured in epi-illumination mode.

Kinetic Analysis

Single-molecule detection and tracking were performed using in-house software [23] and TrackMate [25]. Curve fittings for the kinetic analysis were performed using Origin (Originlab) and Matlab (The MathWorks).

Results

Single-cell Measurements of SOS Dynamics

Using a TIRFM, Halo7-tagged SOS (Halo7-SOS) that was conjugated with tetramethylrhodamine (TMR) (hereafter called "TMR-SOS") was observed as single molecules on the plasma membrane of living HeLa cells (Fig. 2A, Supplementary Movies S1 and S2). In a Western blot analysis, the Halo7-SOS expressed in cells displayed the expected molecular weight (Supplementary Fig. S1A), and accounted for approximately twice as much protein as endogenous SOS (Supplementary Fig. S1B). On incubation of cells with the TMR ligand of Halo7, the association and dissociation of individual TMR-SOS particles with the plasma membrane were detected as the stepwise appearance and disappearance of fluorescence signals, respectively (Fig. 2B). The fluorescence intensities of these particles were similar to the photobleaching step size of molecules that were fixed on the plasma membrane, and few fluorescent particles were observed in cells that lacked expression of Halo7-SOS under the same staining conditions with the TMR ligand (Supplementary Fig. S2A). These results suggest that we were observing behaviors of single SOS molecules. These single molecules of SOS may be incorporated into clusters of SOS molecules [7]. Observation of TMR-SOS with approximately twice fluorescence intensity of single molecules suggests presence of two SOS molecules associate closely. However, more than 85% of the particles were monomeric (Supplementary Fig. S2D). Small but significant amounts of SOS molecules were transiently attached to the plasma membrane before the cells were stimulated with EGF. After stimulation, the density of SOS molecules on the plasma membrane increased, peaking at 3 min, and the increased density preserved, on average, until 8 min (Fig. 2A, C). The time course of SOS translocation was similar to that of RAS activation (Fig. 6). Thus, our single-molecule imaging data support the model in which SOS is expected to be recruited to the plasma membrane as a requirement of Ras activation [4].

In addition to wild-type SOS, we examined a triple mutant of SOS in the REM domain (L687E/R688A/W729E) and a

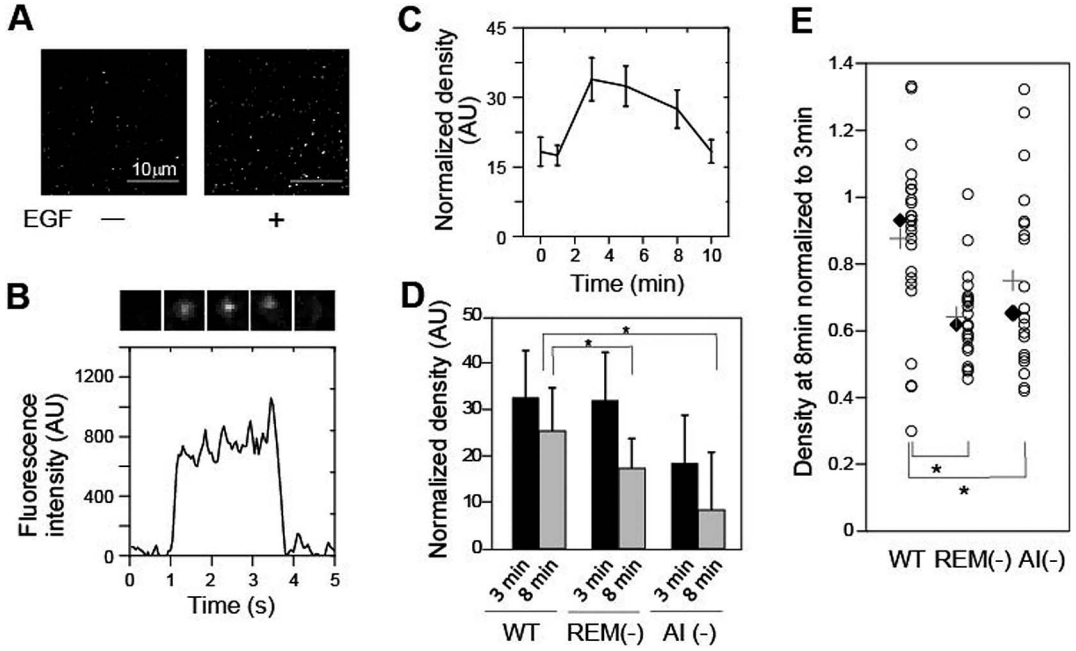

Figure 2 Single-molecule imaging of SOS translocation to the plasma membrane

(A) Snapshots from single-molecule movies of Halo7-SOS (WT) conjugated with tetramethylrhodamine (TMR-SOS). The movies were taken on the plasma membrane of the same living HeLa cell before (left) and after EGF stimulation for 3 min (right). The density of SOS molecules increased after stimulation. (B) A typical single-molecule time course of TMR-SOS on the plasma membrane. The period between the appearance and disappearance of molecules was measured as the dwell time on the plasma membrane. (C) Ensemble-molecule time course of the translocation of WT SOS to the plasma membrane. At time 0, the cells were stimulated with EGF, and the density of TMR-SOS molecules was measured and normalized to SOS expression levels, i.e., TMR fluorescence intensity in the cytoplasm. The mean values for 10 cells were plotted with SE. (D) Increases in SOS density were measured in single cells after EGF treatment for 3 and 8 min, normalized to SOS expression levels, and averaged over 25, 21, and 20 cells expressing WT, REM(–), and AI(–) SOS, respectively. Error bar indicates SE. (*$p<0.05$ on Mann-Whitney test). (E) Ratios of the increases in SOS density at 8 min and 3 min were plotted. The rhombus and plus symbols indicate the average and median values, respectively (*$p<0.05$ on Mann-Whitney test).

single mutant (D140A) in the H domain (Fig. 1A). The wild-type and mutant SOS molecules were designated WT, REM(–), and AI(–), respectively. It has been reported that L687E/R688A and W729E abolish the positive feedback response in SOS-mediated RAS activation [14]. Residue D140 in SOS is conserved between many animal species, from *C. elegans* to humans [7]. In an earlier study, the D140A mutant disrupted the association between the helical linker and H domain [17], which regulates the interaction between RAS-GTP and the REM domain. In a crystal structure, D140 interacts with R552 in the helical linker [8]. Thus, AI(–) is a mutant in the interaction between the H domain and helical linker.

We compared the increases in the density of SOS molecules on the plasma membrane of individual cells at the various times of stimulation with EGF (Fig. 2D). The densities of WT and REM(–) SOS increased similarly after stimulation for 3 min. However, at 8 min, the average increase in REM(–) was significantly less than that of WT. The distribution of SOS densities in individual cells at 8 versus 3 min is plotted in Figure 2E, to detect the sustainability of SOS translocation. Most cells experienced sustained translocation of WT-SOS molecules. However, the majority of cells showed transient translocation of REM(–). This result suggests that the interaction between the REM domain and RAS-GTP is required for the sustained translocation of SOS. The average increases in the density of AI(–) were modest at both 3 and 8 min (Fig. 2D). A population of cells showed sustained translocation of AI(–), but most exhibited transient (and weak) translocation (Fig. 2D, E). It is likely that the AI(–) mutation destabilizes the structure of SOS which is required for its normal association with the membrane components. These data indicate that these mutants of SOS with defects in the positive feedback loop with RAS are also altered in the dynamics of membrane translocation, but that the effects of the mutations are not identical.

Interaction Kinetics of SOS Molecules with the Plasma Membrane

The density of SOS molecules on the plasma membrane is determined by the rates of association and dissociation. First, we measured the dwell times of single SOS molecules on the plasma membrane to determine the dissociation kinetics (Figs. 2B and 3). WT and mutant SOS molecules dissociated from the plasma membrane faster than the photobleaching (Supplementary Fig. S3), indicating rapid turnover of single-

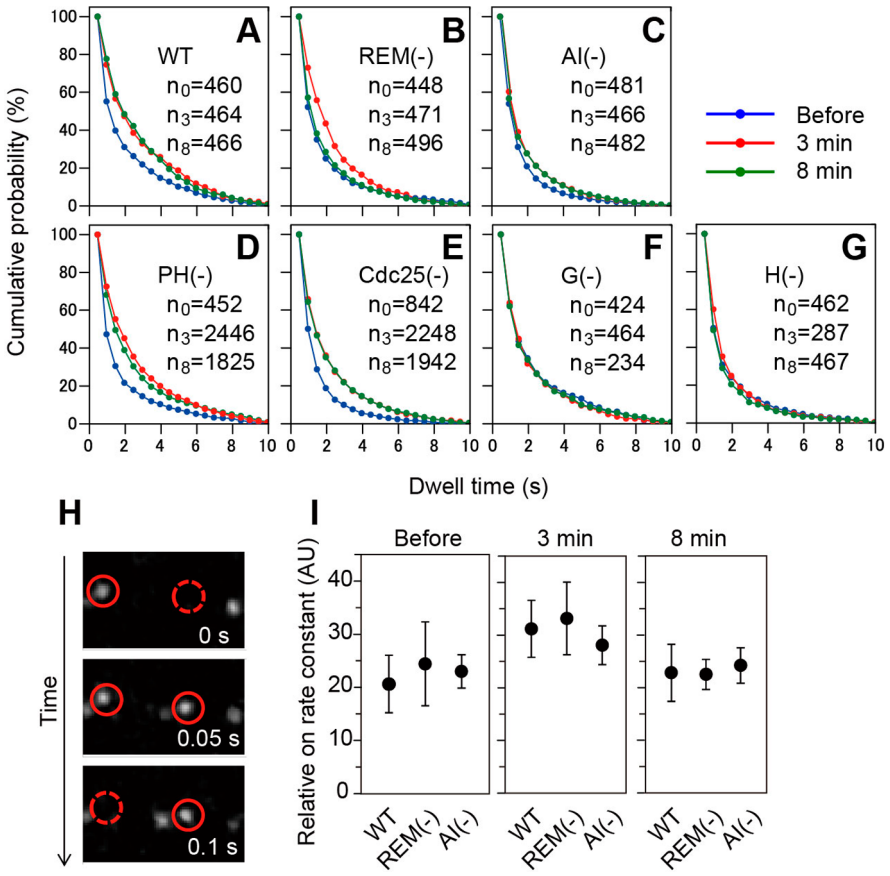

Figure 3 Single-molecule kinetics of SOS molecules with the plasma membrane

(A–G) Typical cumulative distributions of the dwell times for the same single cells before (blue) and after EGF stimulation for 3 min (red) and 8 min (green). The 3-min distributions (red lines) for AI(–) and Cdc25(–) nearly overlap with the 8-min distributions (green lines). n_0, n_3, and n_8 indicate the numbers of fluorescent spots before and after EGF stimulation for 3 and 8 min, respectively, to which the distributions were normalized. (H) Appearance of single SOS molecules on the plasma membrane. (I) The frequency of appearance (number of TMR-SOS molecules per unit time) in the unit area normalized to SOS expression levels (fluorescence intensity of TMR-SOS in the cytoplasm measured in arbitrary units), which is the relative association rate constant. The mean values of the frequencies were measured in 11, 10, and 11 cells expressing WT, REM(–), and AI(–), respectively, and plotted with SE.

molecules of SOS. Turnover of single molecules was much faster than the dynamics of translocation, meaning that the accumulation of SOS on the plasma membrane is maintained as a dynamic equilibrium [23]. The time course of dissociation varied among molecules and periods of EGF stimulation. Compared with the dwell times before stimulation, those of WT molecules were extended after EGF stimulation for 3 min, and this extension was sustained until at least 8 min (Fig. 3A). A similar extension was observed for the dwell times of REM(–) at 3 min, but it was not sustained (Fig. 3B). The dwell times of AI(–) increased only slightly after stimulation with EGF (Fig. 3C). As shown here, in addition to the translocation dynamics (Fig. 2D, E), the dwell times of single SOS molecules on the plasma membrane were affected by mutations in the domains responsible for the positive feedback reaction. Although fluorescence intensity SOS particles were slightly increased after cell stimulation, there were no correlation between the fluorescence intensity and dwell time of single particles (Supplementary Fig. S2D, E).

We examined the domains of SOS that regulate the extension of its dwell times after cell stimulation. SOS contains five putative membrane-binding domains. In addition to REM(–), we constructed four mutants of SOS corresponding to a loss of function in each of the remaining membrane-binding domains (Fig. 1A), and measured their dwell times (Fig. 3D–G). PH(–) and Cdc25(–) had dwell time distributions that were similar to that of WT both before and after EGF stimulation (Fig. 3D, E). Cdc25(–) is inactive, but the activities of endogenous WT SOS could induce dwell time elongation of Cdc25(–). In contrast, the dwell time distributions of G(–) and H(–) did not increase after stimulation even at 3 min (Fig. 3F, G), indicating that these domains coordinate to extend the dwell time of SOS.

Next, we examined the association of SOS molecules by monitoring the appearance of fluorescent particles on the plasma membrane from the cytoplasm (Fig. 3H). To deter-

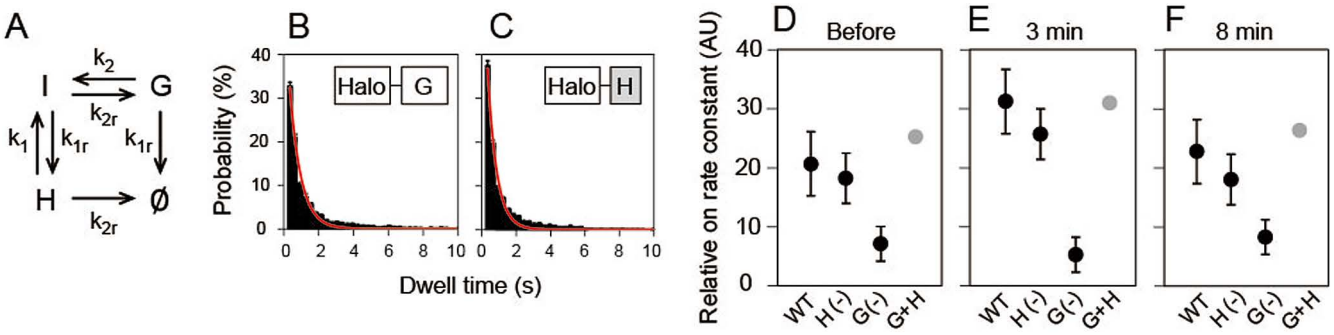

Figure 4 A kinetic model of SOS dissociation

(A) The estimated reaction scheme for SOS dissociation from the plasma membrane. SOS has three association states, G, H, and I. In the G and H states, a SOS molecule associates with the membrane using only the G and H domains, respectively. I is the dissociation intermediate. See text for details. (B, C) The dwell-time distributions of the G (B) and H domains (C) before cell stimulation (bars) were fitted with a single exponential function (red lines). The estimated dissociation rate constants were k_{1r}=1.5 s^{-1} and k_{2r}=1.9 s^{-1}. Similar estimates were obtained when the distributions were fitted after cell stimulation for 3 and 8 min (Supplementary Fig. S3). (D–F) Relative association rate constants for the G and H domains. The mean values±SE. for 11 cells expressing H(–) or G(–) molecules are shown. The same WT data in Figure 3I were plotted as reference. The sums of the rate constants for the H(–) and G(–) molecules (G+H) are also shown.

mine the relative association rate constant, the frequency of appearance per unit time per unit area was measured and normalized to the cytoplasmic fluorescence intensity (in arbitrary unit) reflecting the relative concentration of SOS molecules in the cytoplasm. Residual TMR ligands in cells were negligible (Supplementary Fig. S2A). The relative association rate constants were similar among WT, REM(–), and AI(–) molecules before and at 3 and 8 min of EGF stimulation (Fig. 3I). The rate constants slightly increased from before to after stimulation for 3 min, but this increase was not statistically significant, and nearly returned to basal values at 8 min. Considering the association and dissociation kinetics, we concluded that the REM(–) and AI(–) mutations altered the dynamics of SOS translocation by predominantly affecting the kinetics of dissociation from the plasma membrane.

Kinetic model of SOS dissociation

We constructed a minimal model of SOS dissociation kinetics (Fig. 4A), based on the finding that the G and H domains were solely responsible for extending the dwell times of SOS (Fig. 3) (see Fig. S3 and Supplemental Methods for details). This model contained three association states for SOS (G, H, and I) on the plasma membrane. G or H indicates the association state in which only the G or H domain interacts with the membrane, respectively. I is an intermediate state of dissociation, the formation of which requires both the G and H domains. In the I state, it is possible that the G and H domains associate with the membrane simultaneously, and any other membrane-binding domains and possible interactions between SOS molecules will affect the dwell times during this state. ϕ is the dissociation state in the cytoplasm. In this model, we presumed that the dissociation rate constants of the G and H domains (k_{1r} and k_{2r}, respectively) are independent, i.e., k_{1r} and k_{2r} were common for the dissociations from the I state and from the H and G states. We also presumed that the total number of SOS molecules in cells remains constant. Although this is a coarse-grained model in that various possible structural states of SOS on the plasma membrane were degenerated into three kinetic states, it is the most basic model that can interpret the experimental dwell time distributions (Supplementary Fig. S4), and it provides a simple and unified explanation for the kinetic behaviors of WT and mutant SOS molecules.

We determined the dissociation rate constants for the G (k_{1r}) and H domains (k_{2r}) from the dwell time distributions of SOS fragments that contains the G domain or H domain alone (Fig. 5B, C). Both distributions fit a single-component exponential function well, as assumed in the dissociation model. The estimated dissociation rate constants of the G and H domains were k_{1r} = 1.5 s^{-1} and k_{2r} = 1.9 s^{-1}, respectively, after correction with the photobleaching rate constant (0.05 s^{-1}; Supplementary Fig. S3A, B). These values did not change in cells that were stimulated with EGF (Supplementary Fig. S3C). Dissociation of the G domain from plasma membrane possibly occurs through two pathways, i.e., dissociations of Grb2 from EGFR, and the G domain from Grb2. Single exponential kinetics suggests that one of these two pathways was the rate limiting, though we can not tell which one was that. Another possibility is that the two pathways have similar rate constants. To determine the initial conditions of the model, the relative association rate constants were measured for the G and H fragments (Fig. 4D–F). Before and after (3 and 8 min) SOS activation, the sum of their rate constants approximated to that of WT. REM(–) and AI(–) displayed association rate constants that were similar to those of WT (Fig. 3I). Therefore, we assumed that in the initial association state of SOS [WT, REM(–), and AI(–)] at every stage of cell stimulation, either the G or H domain interacts with the membrane independently at a fractional ratio that is proportional to the association rate constants of the G and H

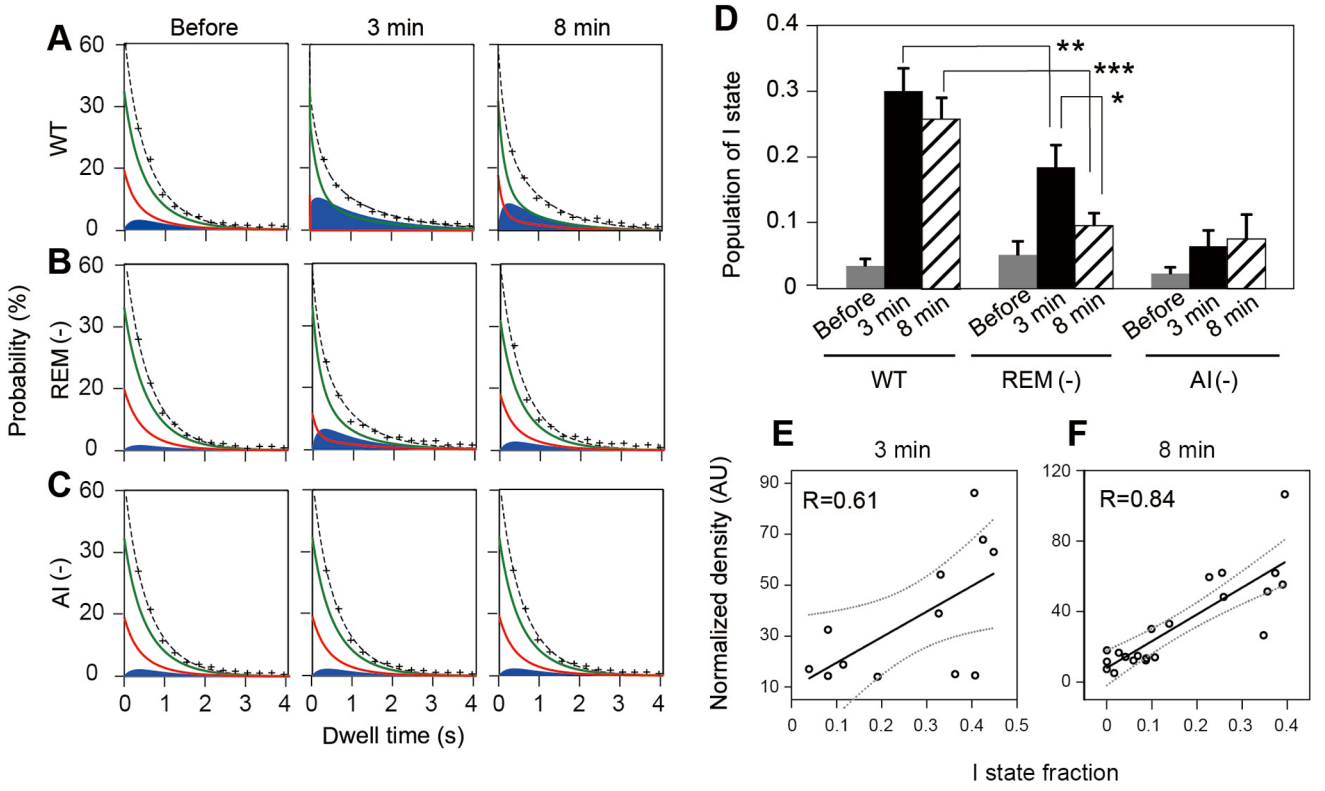

Figure 5 Kinetic analysis of SOS dissociation

(A–C) Typical dwell-time distributions (plus symbols) for the WT (A), REM(–) (B), and AI(–) (C) SOS molecules were fit with the kinetic model in Figure 4A. Lines show the results of fittings for the total (black dotted lines), G (green lines), and H (red lines) states. Blue solids indicate the total fractions of the I state. (D) Fractions of the dissociation intermediate (I) state were estimated in single cells. The mean values±SE for 5 and 9 cells expressing WT SOS (before and after stimulation, respectively); 5, 9, and 7 cells expressing REM(–) (before, 3 min, and 8 min, respectively); and 6 and 5 cells expressing AI(–) (before and after stimulation, respectively) are shown (*$p<0.1$, **$p<0.05$, ***$p<0.01$ on Mann-Whitney test). (E, F) Normalized densities of WT SOS on the plasma membrane plotted against the I state fraction in the dissociation kinetics. Densities were normalized against the expression levels of SOS. Plots were drawn after cell stimulation for 3 (E) and 8 min (F). Open dots indicate values in single cells. Regression lines (solid lines) are shown with their 95% confidence intervals (dotted lines). R indicates the correlation coefficient.

fragments. We estimated that, in the initial association states, the G:H is 0.7:0.3 (before stimulation), 0.8:0.2 (at 3 min), and 0.7:0.3 (at 8 min).

Dissociation Kinetics of SOS from the Plasma Membrane

The dwell time distributions of WT, REM(–), and AI(–) in single cells before and after EGF stimulation for 3 and 8 min (Figs. 3A–C and 5) were fit with the dissociation kinetics model (Fig. 4A) using floating values of k_1 and k_2. As the result, the probability density distributions of the three association states (G, H, and I) were estimated over time after the initial association of the molecule with the plasma membrane (Fig. 5A–C). The fraction of WT molecules that dissociated via the intermediate (I) state increased after EGF stimulation and was sustained for at least 8 min (Fig. 5A). For the REM(–) molecules, the I state fraction was enhanced at 3 min but returned to basal levels at 8 min (Fig. 5B). For the AI(–) molecules, the increase in the I state fraction was small (Fig. 5C). The fraction of the I state during the total dwell times was calculated from the time courses in single cells (Fig. 5D). The I fraction of REM(–) was smaller and less sustained than that of WT, suggesting that the interaction between the REM domain and RAS-GTP takes place during the I state and stabilizes the I state. The small fraction of the I state for AI(–) suggests that the normal orientation between the H domain and helical linker in the WT molecule, which is lost in AI(–), promotes the formation of the I state.

The results of the kinetic analysis suggest that the interaction with RAS at the REM domain regulates the I state fraction but is not required for the I state formation. In addition, the fraction of SOS molecules in the I state corresponds to the membrane density of SOS, correlating with the extension of dwell times. The link between the fraction of the I state and WT SOS density was examined in single cells after stimulation for 3 and 8 min (Fig. 5E, F). We noted a positive correlation at both 3 and 8 min, with a larger correlation coefficient at 8 min (0.84) than at 3 min (0.61), suggesting that at later times, the SOS density on the plasma membrane depends more on the increase in I state, whereas in the early stages, there are mechanisms that increase the dwell time of

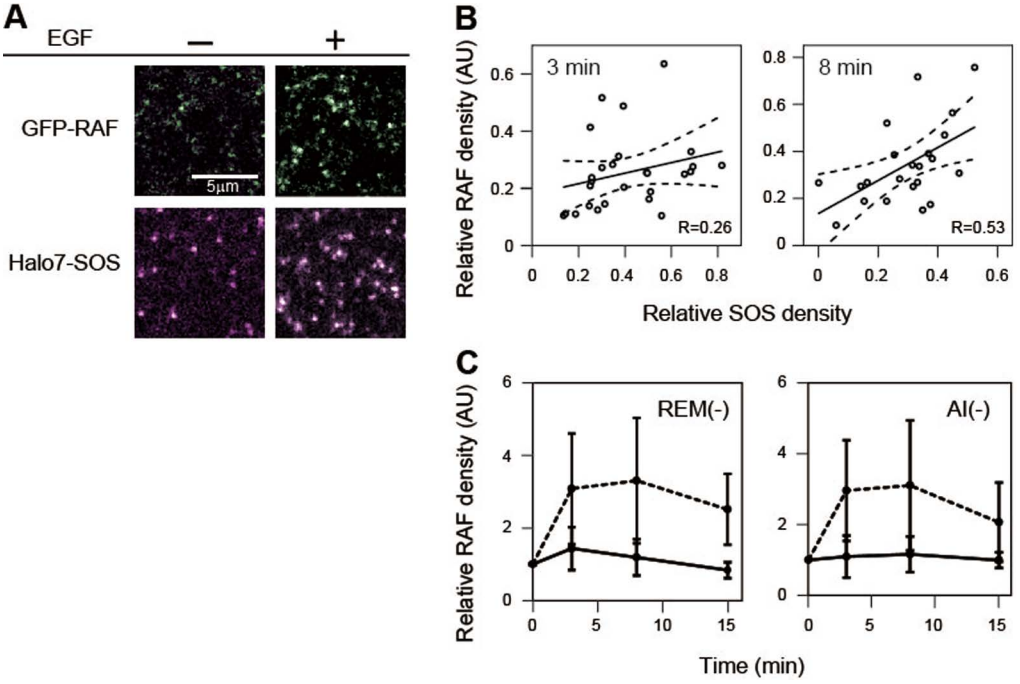

Figure 6 RAS activation detected as the translocation of RAF

(A) Dual-color single-molecule images of GFP-RAF and WT TMR-SOS on the plasma membrane in the same single cell before (–) and after EGF stimulation for 3 min (+). (B) RAF translocation in single cells as a function of WT SOS translocation. Densities of the molecules on the plasma membrane were normalized to the expression levels. Open dots indicate the values in single cells. Regression lines (solid lines) are shown with their 95% confidence intervals (dotted lines). R indicates the correlation coefficient. (C) Time courses of RAF translocation to the plasma membrane in single cells expressing the REM(–) and AI(–) mutants of SOS. Excess amounts of SOS mutants were expressed to examine the dominant negative effects on RAS activation. Cells were stimulated with EGF at time 0. Solid lines indicate the mutants, and dotted lines indicate WT SOS for comparison. The mean values±SE. for 15, 5, and 5 cells expressing WT, REM(–), and AI(–), respectively, are shown.

SOS other than by increasing the I state. An increase in the G state, which has a smaller dissociation rate constant than the H state, at the initial association (Fig. 4E) must be one of these other mechanisms. It is possible that such I-state-independent mechanisms caused the extension in the dwell time of REM(–) at 3 min (Fig. 3B).

SOS/RAS Positive Feedback is Essential for RAF Translocation in Living Cells

To determine how the positive feedback reaction affects downstream reaction, we measured the translocation of SOS and RAF to the plasma membrane in the same cells using dual-color single-molecule imaging (Fig. 6A, Supplementary Movies S3 and S4). RAF is one of the major effector of RAS and recruited from the cytoplasm to the plasma membrane upon RAS activation [26,27]. We transfected cells simultaneously with Halo-7-SOS and GFP-RAF constructs, and monitored the EGF-induced translocation of TMR-SOS and GFP-RAF. Although the correlation was not clear at 3 min, the RAF density tended to be greater in cells with higher SOS densities. After cell stimulation for 8 min, there was a positive correlation between SOS and RAF densities on the plasma membrane (Fig. 6B). Thus, the sustained translocation of SOS to the plasma membrane maintained RAS activation required for RAF translocation. We noted an evident correlation between the fraction of I state and the density of SOS after cell stimulation for 8 min (Fig. 5F). Taken together, the fraction of the I state, and thus the strength of the positive feedback loop between SOS and RAS, is related to the level of RAS activation at 8 min.

The function of the intact positive feedback reaction in RAS activation was noted when we measured the density of RAF on the plasma membrane of cells that expressed excess amounts of REM(–) or AI(–) molecules (Fig. 6C). In these cells, the increase in RAF density after EGF stimulation was nearly abolished. Thus, in living cells, the association of RAS-GTP with the REM domain is required to induce an effective exchange of the nucleotide that is bound to RAS on the Cdc25 domain of SOS, i.e., the positive feedback between SOS and RAS is essential for RAS activation. The normal orientation between the H domain and helical linker in SOS molecules on the plasma membrane is another requirement for SOS function.

Discussion

In this study, we measured the dynamics and kinetics of WT, REM(–), and AI(–) SOS molecules on the plasma mem-

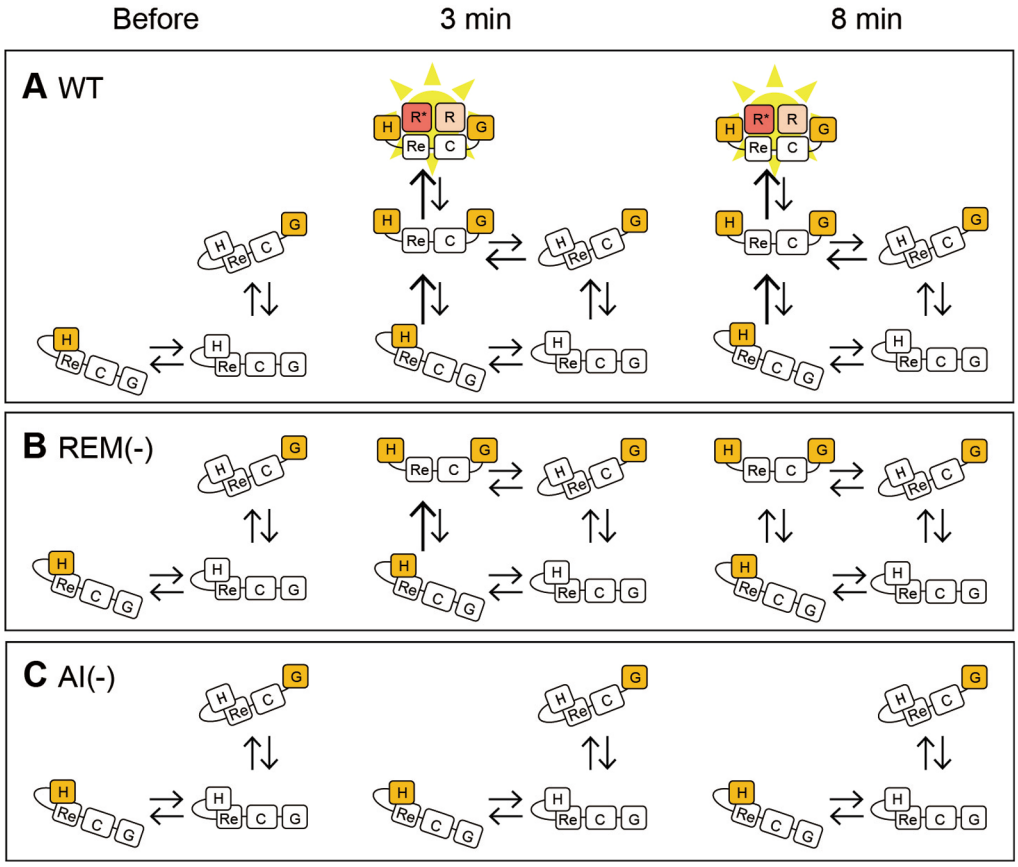

Figure 7 Models of SOS interactions with the plasma membrane
(A) WT SOS in the cytoplasm initially associates with the plasma membrane through either its interaction with activated EGF receptor (G state) or the membrane lipid (H state). In cells stimulated with EGF, a conformational transition then takes place, changing into the dissociation intermediate (I state). The I state can be a mixture of multiple substates, in which other membrane-associating domains (PH, REM, and Cdc25) of SOS are involved. During the I state, the REM domain interacts with the positive feedback RAS, and the GEF activity of SOS is stimulated. (B) REM(–) SOS takes the I state, but because it does not interact with positive feedback RAS, its GEF activity is not stimulated. (C) AI(–) SOS cannot assume the I state. See text for details. Re, C, R, and R* indicates the REM domain, Cdc25 domain, RAS-GTP, and RAS-GDP, respectively.

branes of living HeLa cells stimulated with EGF. Based on the kinetic analysis of the dwell times of the SOS molecules on the membrane, we identified an intermediate (I) dissociation state and formulated the function and dynamics of SOS in RAS activation, based on the fraction of the I state. Through this intermediate state, the positive feedback loop between SOS and RAS that was identified in biochemical *in vitro* experiments was shown to function in the context of living cells. The positive feedback loop is critical for RAS/RAF signal transduction in living cells.

The dwell time analysis of SOS on the plasma membrane suggests that the both G and H domains are required for formation of the I state, which was detected based on the extension of the dwell time (Fig. 3). Simultaneous associations of two domains bring a non-linearity in the I state formation, making the I state as a switch of SOS-mediated RAS activation. The interaction between SOS and RAS-GTP (feedback RAS) at the REM domain stabilizes the I state, as shown form the extended dwell times of WT more than that of REM(–). However, this interaction was not necessary for I state formation, because the I state also occurred with the REM(–) mutant (Fig. 5D). In the early stages (3 min) of EGF stimulation, an increase of the association rate constants k_1 and k_2 resulted in the large I state fraction in WT and REM(–) molecules (Supplementary Fig. S5). This increase must have been caused by the activation of EGFR that produces GRB2-binding sites on the EGFR molecules and increases the density of acidic phosphatidylinositol phosphates via the activation of PI3Ks. Stabilization of the I state by other membrane association domains of SOS, including REM, also results in the increase of k_1 and k_2 in this simple kinetic model. At 8 min, the fraction of I state was greater in WT than in REM(–) (Fig. 5D), suggesting that WT SOS interacts with the feedback RAS during the I state. This interaction is not shown in the reaction scheme (Fig. 4A), but Figure 7 illustrates our model of SOS dynamics on the plasma membrane, including the interactions of SOS with RAS molecules. The accumulation of RAS-GTP on the plasma membrane after EGF stim-

ulation might sustain the I state fraction in WT (Fig. 5D).

In the AI(–) mutant, the fraction of I state was modest at both 3 and 8 min of cell stimulation (Fig. 5D), and this mutation, nearly completely inhibited RAF translocation and thus, the activation of RAS (Fig. 6C). These data suggested that signal dependent conformation change is abnormal in AI(–). In the crystal structure, D140 and D169 interact with R552 to stabilize the association between the H domain and helical linker [8]. In the R552G mutant, which has been identified in Noonan syndrome [18], the interaction between the H domain and helical linker will be lost, implicating R552G as a hyper-active mutant. In contrast, in the AI(–) (D140A) mutant, the interaction between D169 and R552 could be remained. Therefore, one explanation of our results is that in the AI(–) mutant, the autoinhibition conformation is maintained in the H and G states, but the normal orientation between the H and G domains is lost by D140A mutation, preventing the simultaneous association of these two domains with the plasma membrane. Inhibition of the formation of the I state in AI(–) should cause its function to be lost in RAS activation, which requires the positive feedback loop between SOS and RAS. This might be why D140A has not been identified in Noonan syndrome. This possibility must be examined in future studies.

The mechanism of positive feedback between SOS and RAS-GTP is not precisely known. Since isolated Cdc25 domain of SOS targeted to the plasma membrane by tagging with a CAAX motif has been reported to be active [28], it is possible that the REM domain is inhibitory for the GEF activity in the Cdc25 domain and association of RAS-GTP with the REM domain releases this inhibition. Then, the role of I state formation is to change the SOS structure to allow the release of inhibition. Another possibility is that elongated membrane association of Cdc25-CAAX was sufficient for RAS activation. In this case, dwell time elongation by the concerted function of H, G, and REM domains is critical for WT SOS to activate RAS.

The sustained translocation of SOS in cells seems to require the positive feedback loop between SOS and RAS, because it is lost in REM(–) and AI(–) (Fig. 2E). But, how the molecular kinetics sustains this translocation in ensemble molecule dynamics is unknown. If the positive feedback loop between SOS and RAS functions autonomously, it will induce continuous activation of RAS. However, in steady-state dynamics, although the accumulation of RAS-GTP (feedback RAS) on the cell surface increases the proportion of active SOS in the I state as shown in our kinetic model (Fig. 7A), SOS activity will return to basal levels unless RAS-GTP also induces the translocation of SOS to the membrane [15]. Because the REM(–) mutant did not have a lower association rate with the membrane (Fig. 3), it is improbable that RAS-GTP increases the translocation of SOS under the conditions in living cells stimulated with EGF. We observed a slightly higher association rate constant for WT SOS with the membrane after stimulation for 8 min versus before stimulation (Fig. 3), but the difference was not statistically significant. Therefore, the sustained translocation of SOS might not be a quasi-steady state, but slow transient dynamics.

Regardless of the mechanism that sustains the SOS/RAS feedback, the positive feedback loop between SOS and RAS is not merely regulatory but is critical for RAS activation (Fig. 6C). This requirement for the positive feedback loop inevitably results in a nonlinear switch-like input-output relationship between SOS translocation and RAS activation. This response of the SOS-RAS system is advantageous in preventing spontaneous mis-activation and in amplification of small signals below critical levels. Yet, simultaneously, it might induce large cell-to-cell deviations with similar inputs when the small differences in the initial and/or boundary conditions are amplified. It is likely that the wide cell-to-cell variability in the sustained translocation of WT SOS (Fig. 2E) is caused by the positive feedback loop. In contrast, negative feedback from ERK, which is activated downstream of RAF and phosphorylates the G domain of SOS to prevent interaction with GRB2 [29], is a mechanism that might impede SOS translocation at the later stage (>8 min) of cell stimulation.

In conclusion, this study indicates that an intermediate state formation functions as a switch of SOS activity, corresponding to the establishment of the positive feedback loop between SOS and RAS. The multiple membrane-associating domains of SOS, particularly the H, REM, and G domains, function in concert during the intermediate state of membrane association, in which SOS interacts with the feedback RAS molecule to be a fully active GEF for RAS. Because the activation of RAS requires the positive feedback domains of SOS, the SOS/RAS positive feedback is crucial in regulating the diverse functions of growth factors that lie upstream of SOS. Various point mutations in SOS induce disease, including cancer and RAS-RAF syndromes [30]. Some of these mutations have been detected in SOS domains that do not directly control nucleotide exchange on RAS, and their pathological mechanisms are unclear. Our study raises the possibility that these mutations affect SOS function by altering the coordination among multiple SOS domains.

Acknowledgments

We thank Dafna Bar-Sagi, New York University School of Medicine for the pCGM-HA-hSos1 plasmid and Hiromi Sato for technical assistance. Y. N. was supported by a Junior Research Associate (JRA) grant from RIKEN.

Conflicts of Interst

All authors declare that they have no conflict of interest.

Author Contributions

T. Y. and Y. S. designed the study. Y. N. and K. H. performed the experiments and analyzed the data. Y. N., K. H., and Y. S. wrote the manuscript.

References

[1] Simon, M. A., Bowtell, D. D. L., Dodson, G. S., Laverty, T. R. & Rubin, G. M. Ras1 and a putative guanine nucleotide exchange factor perform crucial steps in signaling by the sevenless protein tyrosine kinase. *Cell* **67**, 701–716 (1991).

[2] Olayioye, M. A., Neve, R. M., Lane, H. A. & Hynes, N. E. The ErbB signaling network: receptor heterodimerization in development and cancer. *EMBO J*. **19**, 3159–3167 (2000).

[3] Chardin, P., Camonis, J. H., Gale, N. W., Aelst, L. V., Schlessingler, J., Wingler, M. H., *et al*. Human Sos1: a guanine nucleotide exchange factor for Ras that binds to GRB2. *Science* **260**, 1338–1343 (1993).

[4] Aronheim, A., Engeliberg, D., Li, N., Al-Alawi, N., Schlessinger, J. & Karin, M. Membrane targeting of the nucleotide exchange factor Sos is sufficient for activating the Ras signaling pathway. *Cell* **78**, 949–961 (1994).

[5] Milburn, M. V., Tong, L., Devos, A. M., Brunger, A., Yamaizumi, Z., Nishimura, S., *et al*. Molecular switch for signal transduction: structural differences between active and inactive forms of protooncogenic ras proteins. *Science* **247**, 939–945 (1990).

[6] Boriack-Sjodin, P. A., Margarit, S. M., Bar-sagi, D. & Kuriyan, J. The structural basis of the activation of Ras by Sos. *Nature* **394**, 337–343 (1998).

[7] Sondermann, H., Soisson, S. M., Bar-Sagi D. & Kuriyan, J. Tandem histone folds in the structure of the N-terminal segment of the Ras activator Son of Sevenless. *Structure* **11**, 1583–1593 (2003).

[8] Gureasko, J., Kuchment, O., Makino, D. L., Sondermann, H., Bar-Sagi, D. & Kuriyan, J. Role of the histone domain in the autoinhibition and activation of the Ras activator Son of Sevenless. *Proc. Natl. Acad. Sci. USA* **107**, 3430–3435 (2010).

[9] Yadav, K. K. & Bar-Sagi, D. Allosteric gating of Son of sevenless activity by the histone domain. *Proc. Natl. Acad. Sci. USA* **107**, 3436–3440 (2010).

[10] Chen, R.-H., Corbalan-Garcia, S. & Bar-Sagi, D. The role of the PH domain in the signal-dependent membrane targeting of Sos. *EMBO J*. **16**,1351–1359 (1997).

[11] Zhao, C., Du, G., Skowronek, K., Frohman, M. A. & Bar-Sagi, D. Phospholipase D2-generated phosphatidic acid couples EGFR stimulation to Ras activation by Sos. *Nat. Cell Biol*. **9**, 707–712 (2007).

[12] Yang, S., Aelst, L. V. & Bar-Sagi, D. Differential interactions of human Sos1 and Sos2 with Grb2. *J. Biol. Chem*. **270**, 18212–18215 (1995).

[13] Margarit, S. M., Sondermann, H., Hall, B. E., Nagar, B., Hoelz, A., Pirruccello, M., *et al.* Structural evidence for feedback activation by Ras·GTP of the Ras-specific nucleotide exchange factor SOS. *Cell* **112**, 685–695 (2003).

[14] Sondermann, H., Soisson, S. M., Boykevisch, S., Yang, S.-S, Bar-Sagi, D. & Kuriyan, J. Structural analysis of autoinhibition in the Ras activator Son of sevenless. *Cell* **199**, 393–405 (2004).

[15] Hall, B. E., Yang, S. S., Boriack-Sjodin, P. A., Kuriyan, J. & Bar-Sagi, D. Structure-based mutagenesis reveals distinct functions for Ras switch 1 and swich2 in Sos-catalyzed Guanine Nucleotide Exchange. *J. Biol. Chem*. **276**, 27629–27637 (2001).

[16] Das, J., Ho, M., Zikherman, J., Govern, C., Yang, M., Weiss, A., *et al.* Digital signaling and hysteresis characterize Ras activation in lymphoid cells. *Cell* **136**:337–351 (2009).

[17] Sondermann, H., Nagar, B., Bar-Sagi, D. & Kuriyan, J. Computational docking and solution x-ray scattering predict a membrane-interacting role for the histone domain of the Ras activator son of sevenless. *Proc. Natl. Acad. Sci. USA* **102**, 16632–16637 (2005).

[18] Roberts, A. E., Araki, T., Swanson, K. D., Montgomery, K. T., Schiripo, T. A., Joshi, V. A., *et al.* Germline gain-of-function mutations in SOS1 cause Noonan syndrome. *Nat. Genetics* **39**, 70–74 (2006).

[19] Iversen, L., Tu, H., Lin, W., Cristensen, S. M., Abel, S. M., Iwig, J., *et al.* Ras activation by SOS: allosteric regulation by altered fluctuation dynamics. *Science* **345**, 50–54 (2014).

[20] Matsuoka, S., Iijima, M., Watanabe, T. M., Kuwayama, H., Yanagida, T., Devreotes, P. N., *et al.* Single-molecule analysis of chemoattractant-stimulated membrane recruitment of a PH-domain-containing protein. *J. Cell Sci.* **119**, 1071–1079 (2006).

[21] Hibino, K., Shibata, T., Yanagida, T. & Sako, Y. Ativation kinetics of RAF protein in the ternary complex of RAF, RAS-GTP, and kinase on the plasma membrane of living cells. *J. Biol. Chem*. **286**, 36460–36468 (2011).

[22] Hiroshima, M., Saeki, Y., Okada-Hatakeyama, M. & Sako, Y. Dynamically varying interactions between heregulin and ErbB proteins detected by single-molecule analysis in living cells. *Proc. Natl. Acad. Sci. USA* **109**, 13984–13989 (2012).

[23] Hibino, K., Watanabe, T. M., Kozuka, J., Hikikoshi-Iwane, A., Okada, T., Kataoka, T., *et al.* Single- and multiple-molecule dynamics of the signaling from H-Ras to cRaf-1 visualized on the plasma membrane of living cells. *Chem. Phys. Chem.* **4**, 748–753 (2003).

[24] Hibino, K., Hiroshima, M., Takahashi, M. & Sako, Y. Single-molecule imaging of fluorescent proteins expressed in living cells. *Methods Mol. Biol*. **48**, 451–460 (2009).

[25] Jaqaman, K., Loerke, D., Mettle, M., Kuwata, H., Grinstein, S., Schmid, S. L. & Danuser, G. Robust single-particle tracking in live-cell time-lapse sequences. *Nat. Methods* **5**, 695–702 (2008).

[26] Leevers, S. J., Paterson, H. F. & Marshall, C. J. Requirement for Ras in Raf activation is overcome by targeting Raf to the plasma membrane. *Nature* **369**, 411–414 (1994).

[27] Stokoe, D., Macdonald, S. G., Cadwallader, K., Symons, M. & Hancock, J. F. Activation of Raf as a result of recruitment to the plasma membrane. *Science* **264**, 1463–1467 (1994).

[28] Quilliam, L. A., Huff, S. Y., Rabun, K. M., Wei, W., Park, W., Broek, D., *et al.* Membrane-targeting potentiates guanine nucleotide exchange factor CDC25 and SOS1 activation of Ras transforming activity. *Proc. Natl. Acad. Sci. USA* **91**, 8512–8516 (1994).

[29] Corbalan-Garcia, S., Yang, S. S., Degenhardt, K. R. & Bar-Sagi, D. Identification of the mitogen-activated protein kinase phosphorylation sites on human Sos1 that regulate interaction with Grb2. *Mol. Cell Biol*. **16**, 5674–5682 (1996).

[30] Lepri, F., Luca, A. D., Stella, L., Rossi, C., Baldassarre, G., Pantaleoni, F., *et al.* SOS1 mutations in Noonan syndrome: molecular spectrum, structural insights on pathogenic effects, and genotype–phenotype correlations. *Hum. Mutat*. **32**, 760–772 (2011).